

MEMORY ENCODING IN AMYGDALA

by

Chen Yan

A thesis submitted in conformity with the requirements
for the degree of Doctor of Philosophy
Institute of Medical Science
University of Toronto

© Copyright 2016 by Chen Yan

ABSTRACT

Memory Encoding in Amygdala

Chen Yan

Doctor of Philosophy

Institute of Medical Science

University of Toronto

2016

Lorem ipsum dolor sit amet, consectetuer adipiscing elit. Ut purus elit, vestibulum ut, placerat ac, adipiscing vitae, felis. Curabitur dictum gravida mauris. Nam arcu libero, nonummy eget, consectetuer id, vulputate a, magna. Donec vehicula augue eu neque. Pellentesque habitant morbi tristique senectus et netus et malesuada fames ac turpis egestas. Mauris ut leo. Cras viverra metus rhoncus sem. Nulla et lectus vestibulum urna fringilla ultrices. Phasellus eu tellus sit amet tortor gravida placerat. Integer sapien est, iaculis in, pretium quis, viverra ac, nunc. Praesent eget sem vel leo ultrices bibendum. Aenean faucibus. Morbi dolor nulla, malesuada eu, pulvinar at, mollis ac, nulla. Curabitur auctor semper nulla. Donec varius orci eget risus. Duis nibh mi, congue eu, accumsan eleifend, sagittis quis, diam. Duis eget orci sit amet orci dignissim rutrum.

Nam dui ligula, fringilla a, euismod sodales, sollicitudin vel, wisi. Morbi auctor lorem non justo. Nam lacus libero, pretium at, lobortis vitae, ultricies et, tellus. Donec aliquet, tortor sed accumsan bibendum, erat ligula aliquet magna, vitae ornare odio metus a mi. Morbi ac orci et nisl hendrerit mollis. Suspendisse ut massa. Cras nec ante. Pellentesque a nulla. Cum sociis natoque penatibus et magnis dis parturient montes, nascetur ridiculus mus. Aliquam tincidunt urna. Nulla ullamcorper vestibulum turpis. Pellentesque cursus luctus mauris.

Nulla malesuada porttitor diam. Donec felis erat, congue non, volutpat at, tincidunt tristique, libero. Vivamus viverra fermentum felis. Donec nonummy pellentesque ante. Phasellus adipiscing semper elit. Proin fermentum massa ac quam. Sed diam turpis, molestie vitae, placerat a, molestie nec, leo. Maecenas lacinia. Nam ipsum ligula, eleifend at, accumsan nec, suscipit a, ipsum. Morbi blandit ligula feugiat magna. Nunc eleifend consequat lorem. Sed lacinia nulla vitae enim. Pellentesque tincidunt purus vel magna. Integer non enim. Praesent euismod nunc eu purus. Donec bibendum quam in tellus. Nullam cursus pulvinar lectus. Donec et mi. Nam vulputate metus eu enim. Vestibulum pellentesque felis eu massa.

Quisque ullamcorper placerat ipsum. Cras nibh. Morbi vel justo vitae lacus tincidunt ultrices. Lorem ipsum dolor sit amet, consectetuer adipiscing elit. In hac habitasse platea dictumst. Integer tempus convallis augue. Etiam facilisis. Nunc elementum fermentum wisi. Aenean placerat. Ut imperdiet, enim sed gravida sollicitudin, felis odio placerat quam, ac pulvinar elit purus eget enim. Nunc vitae tortor. Proin tempus nibh sit amet nisl. Vivamus quis tortor vitae risus porta vehicula.

ACKNOWLEDGEMENTS

Lorem ipsum dolor sit amet, consectetuer adipiscing elit. Ut purus elit, vestibulum ut, placerat ac, adipiscing vitae, felis. Curabitur dictum gravida mauris. Nam arcu libero, nonummy eget, consectetuer id, vulputate a, magna. Donec vehicula augue eu neque. Pellentesque habitant morbi tristique senectus et netus et malesuada fames ac turpis egestas. Mauris ut leo. Cras viverra metus rhoncus sem. Nulla et lectus vestibulum urna fringilla ultrices. Phasellus eu tellus sit amet tortor gravida placerat. Integer sapien est, iaculis in, pretium quis, viverra ac, nunc. Praesent eget sem vel leo ultrices bibendum. Aenean faucibus. Morbi dolor nulla, malesuada eu, pulvinar at, mollis ac, nulla. Curabitur auctor semper nulla. Donec varius orci eget risus. Duis nibh mi, congue eu, accumsan eleifend, sagittis quis, diam. Duis eget orci sit amet orci dignissim rutrum.

Nam dui ligula, fringilla a, euismod sodales, sollicitudin vel, wisi. Morbi auctor lorem non justo. Nam lacus libero, pretium at, lobortis vitae, ultricies et, tellus. Donec aliquet, tortor sed accumsan bibendum, erat ligula aliquet magna, vitae ornare odio metus a mi. Morbi ac orci et nisl hendrerit mollis. Suspendisse ut massa. Cras nec ante. Pellentesque a nulla. Cum sociis natoque penatibus et magnis dis parturient montes, nascetur ridiculus mus. Aliquam tincidunt urna. Nulla ullamcorper vestibulum turpis. Pellentesque cursus luctus mauris.

CONTENTS

1. Introduction	1
2. Literature Review	2
2.1. Hypothesis and Research Aims	2
3. General Methods	3
3.1. Mice	3
3.2. Viral Infusion	3
3.3. Histology	3
3.4. Behavioural Experiments	4
3.4.1. Auditory fear conditioning	4
3.4.2. Cocaine-conditioned place preference	4
3.4.3. Animal tracing	5
4. Memory traces in amygdala	6
4.1. Introduction	6
4.2. Methods	6
4.2.1. Animals	6
4.2.2. Viral vectors	6
4.2.3. Surgery	6
4.2.4. Auditory fear conditioning	6
4.2.5. Cocaine-conditioned place preference	7
4.2.6. Flourescent <i>in situ</i> hybridization	7
Tissue preparation	7
Riboprobe synthesis	7
Hybridization and staining	7
Analysis	8
4.3. Results	8
4.4. Discussion	11

5. Construction of a miniature epi-fluorescence microscope	12
5.1. Introduction	12
5.2. Material and Methods	13
5.2.1. Design of the mini-microscope	13
Lens configuration	13
Filter selection	14
Electronics	14
Casing and assembly	14
Objective lens assembly for deep brain imaging	15
5.2.2. Implantation of the mini-microscope	16
5.2.3. In vivo mini-microscope testing	16
5.2.4. Image analysis	16
Illumination correction	16
Motion correction	16
Extracting cell from calcium imaging video	16
Mapping cells across session	17
5.3. Results	17
5.3.1. mini-microscope	17
5.3.2. Video preprocessing	20
illumination correction	20
motion correction	20
5.3.3. Measuring blood flow with mini-microscope	21
5.3.4. Recording calcium transients in CA1	22
5.3.5. between session stability	27
5.3.6. Deep brain imaging	27
5.3.7. Two colour	27
5.4. Discussion	29
6. Dynamics of neural network in amygdala during memory formation	30
7. General Discussion	31
8. Conclusions and Future Directions	32
Bibliography	33
A. Appendix	34
A.1. Code	34

LIST OF TABLES

LIST OF FIGURES

5.2.	(a) Schematic of the miniature microscope. Excitation light is emitted from a high-intensity blue LED, filtered and reflected to the sample by a dichroic mirror. GCaMP6 emission is collected by the gradient-index (GRIN) lens, filtered and focused onto a CMOS camera chip, where the images are sent to a computer and recorded. (b) Prototype of the mini-microscope. (c) USAF resolution test target under the mini-microscope.	19
5.3.	, before, after	20
5.4.	<i>In vivo</i> image of blood vessel. The animal received 10mg/kg fluorescein-dextran in tail vein. The mini-microscope is placed at cortex when the animal is under anaesthesia.	22
5.5.	Cells in CA1 captured by the mini-microscope in behaving animal. Two weeks after AAV infusion and microscope implantation, the animal is allowed to freely explore a novel environment. The picture is a maximum projection of all frames captured in a 5-minute session.	23
5.6.	Example of an independent component of the movie after analysis, showing both the extracted spatial location of the cell (left) and the un-normalized activity (top right).	24
5.7.	More than 100 cells are identified in a single imaging session. The identified cells are randomly coloured.	25
5.8.	Activity of 4 sample cells plotted against location of the animal. The colour represents the Ca^{2+} activity. The cellular activity is specific to the animal's location in the environment.	26
5.9.	Raw calcium signals during fear conditioning. Left: extracted map of neurons, randomly coloured. Right: Sample calcium signals over time.	27
5.10.	Images of cells with different fluorescent protein under the two-colour mini-microscope prototype. (a) HSV-GFP in perfused brain. (b) HSV-tdTomato in perfused brain. (c) Red retrobeads <i>in vivo</i> in green channel. (d) Red retrobeads <i>in vivo</i> in red channel.	28

GLOSSARY

A/P anteroposterior

AAV adeno-associated virus

AFC auditory fear conditioning

Arc activity-regulated cytoskeleton-associated protein

CA1 cornu ammonis area 1

cDNA complimentary DNA

CMOS complimentary metal-oxide-semiconductor

CMV cytomegalovirus

CPP cocaine-conditioned place preference

CREB cyclic adenosine monophosphate response binding protein

D/V dorsoventral

DC direct current

DIG digoxigenin

DNA deoxyribonucleic acid

EDTA ethylenediaminetetraacetic acid

FDM fused deposition modelling

FISH flourescent *in situ* hybridization

FITC flourescein isothiocyanate

GFP green fluorescence protein

GRIN gradient-index

HRP horseradish peroxidase

HSV herpes simplex virus

ICA independent component analysis

IEG immediately-early gene

i.p. intraperitoneal

LA lateral amygdala

LED light-emitting diode

M/L mediolateral

NAc nucleus accumbens

PBS phosphate-buffered saline

PCA principle component analysis

PFA paraformaldehyde

PLA polylactic acid

RNA ribonucleic acid

SSC buffer saline sodium citrate buffer

TRITC tetramethylrhodamine

TSA tyramide signal amplification

USAF United States Air Force

USB universal serial bus

UV ultraviolet

TODO LIST

vibrotome info	4
permaflour info	4
Nikon info	4
insert cpp image here	4
Animal tracing method	5
refer to general methods	6
refer to general methods	6
refer to general methods	7
description why catfish	7
info about OCT compound	7
right way to put this	7
in vitro transcription detail	7
labeling mix detail	7
RNA column info	7
prehyb info	7
Ab info	8
Ab info	8
edit microscope intro	12
maybe a illustration	13
GoFoton lens info	14
GoFoton lens info	14
chroma filter info	14
chroma filter info	14
slipring info	14
Video capture info	14
reference code	14
led info	14
DC power source info	14
info side screw	15
microscope body nut spec	15

epoxy info?	15
baseplate thread tube info	15
clamp details	15
manipulator details	15
insert figure for the setup	15
uv light source info	15
ref general methods	16
coordinate for ca1 and amygdala	16
illumination correction meth	16
motion correction meth	16
ref TrimICP	17
mouse image?	17
insert microscope photo and mouse figure here	17
USAF target detail	17
Figure: animal with scope	18
Nikon details	18
insert Nikon image	18
reorganize figures	18
move to methods?	20
... and nomalized by multiplying the inverse of the difference of illumination pattern to roof	20
image	20
Figure: before correction	20
Figure: after correction	20
reference opencv?	20
ref max projection image	21
Figure: max projection, x/y motion plot	21
calculating blood flow	21
image, blood vessel detection, velocity heatmap	21
max projection, sample cell, animal tracing, place cell heat map	22
alignment figure	27
alignment result, how many percentage overlap??	27
figure matching cells across sessions	27
same as CA1 analysis	27
retrobeads info	27
wording	27

1

INTRODUCTION

2

LITERATURE REVIEW

50+ pages

2.1 Hypothesis and Research Aims

2-5 pages

3

GENERAL METHODS

3.1 Mice

Wildtype C57/BL6 × 129 F1 mice of 3-months age were used in the experiments. All animals were caged in groups of 4 or 5, with a 12-hour light/dark cycle. All experiments are performed during the light phase of the cycle. Food and water are provided *ad libitum* to all animals. All procedures are approved by the Animal Care and Use Committee in the Hospital for Sick Children.

3.2 Viral Infusion

Each animal received intraperitoneal (i.p.) injection of atropine (0.1 mg kg^{-1}) and chlorhydrate (400 mg kg^{-1}) before being secured on a stereotaxic frame. An incision was made on the scalp and the skin was pulled to the side to reveal the skull. Holes were drilled above lateral amygdala (LA) on the skull for micropipette injection. Virus was loaded into a glass micropipette and gradually lowered to target coordinate. $1.5 \mu\text{l}$ of virus were injected on each side at a rate of $0.12 \mu\text{l}/\text{min}$, aiming at LA (anteroposterior (A/P) -1.4 mm , medio-lateral (M/L) $\pm 3.5 \text{ mm}$, dorsoventral (D/V) 5.0 mm from Bregma). The micropipette was left in the brain for an extra 10 min before slowly retracted. The incision was sutured and treated with antibiotics. Each animal then received subcutaneous injection of analgesic (ketoprofen, 5 mg kg^{-1}) before returned to a partially heated clean cage for recovery. All behaviour experiments are conducted at least 3 days after surgery.

3.3 Histology

Placement of implants and extent of viral infections was determined by green fluorescence protein (GFP) expression. After all experiments, animals were transcardially perfused with

first phosphate-buffered saline (PBS) then 4% paraformaldehyde (PFA). The brains were dissected and kept in 4% PFA overnight, and washed with PBS. The brains were then sliced coronally on a vibrotome () to 50 µm thickness. Slices containing LA were then mounted on gelatin-coated glass slices with a hardening mounting media (Permaflour) and assessed under an epi-fluorescence microscope(Nikon).

vibrotome info
permaflour info
Nikon info

3.4 Behavioural Experiments

3.4.1 Auditory fear conditioning

The auditory fear conditioning (AFC) chamber (Med Associates) consists of two plexiglass walls and two metal walls, with an overhead camera for recording animal behaviour and a metal grid floor for shock delivery. The chamber was cleaned with water before AFC training. The animals were placed in the chamber and allowed for a 2-minute habituation. A tone (2800 Hz, 85 dB) was played for 30 s and co-terminated with a 2-second shock (0.7 mA). The animals were returned to their home cage 30 s after the shock.

The AFC chamber is modified for testing by inserting a plexiglass board horizontally to cover the metal grids, and two more boards vertically to meet at the rear of the chamber, creating a triangular space. The testing chamber is washed with 70% ethanol. During testing, animals were placed in the triangular space. A 1 min tone was played 2 min after the animal was put in the chamber. The amount of freezing was assessed.

3.4.2 Cocaine-conditioned place preference

The cocaine-conditioned place preference (CPP) boxes are composed of two chambers with a removable shutter that can be switched to allow animals to move between the chambers. One chamber has white walls, textured floor and is sprayed with water, the other chamber has striped walls, smooth floor and is sprayed with 2% acetic acid. Animals were first placed in the box, allowed to travel between two chambers for 10 min, and the amount of time spent in each chamber is recorded as a measure for pre-conditioning preference. During training, animals received saline (i.p.), and confined to one of the chambers for 15 min. In the next day, the animals received cocaine injection (30 mg kg^{-1} , i.p.), and paired to the other chamber for 15 min. The animals are kept in home cage for one day and put back to the CPP boxes and allowed to move freely between chambers for 10 min. The amount of time spent in each chamber were recorded. The difference in time spent between cocaine and saline conditioned chamber were calculated as cocaine preference.

insert cpp image here

3.4.3 Animal tracing

Animal
tracing
method

4

MEMORY TRACES IN AMYGDALA

4.1 Introduction

4.2 Methods

4.2.1 Animals

Wildtype C57/BL6 × 129 F1 mice of 3-month age were used in the experiment. All animals were caged in groups of 4 or 5, with a 12-hour light/dark cycle. Food and water are provided *ad libitum* to all animals.

4.2.2 Viral vectors

p1005 plasmid expresses GFP under cytomegalovirus (CMV) promoter. CREB–p1005–GFP plasmid was constructed by inserting cyclic adenosine monophosphate response binding protein (CREB) complimentary DNA (cDNA) into p1005 plasmid, under the control of herpes simplex virus (HSV) IE4/5 promoter. Plasmids were packaged with a replication-defective HSV helper virus as previously described (Neve et al., 2005). All virus was concentrated by sucrose gradient, diluted in 10% sucrose and stored in –80 °C. A typical titer of the virus is 1×10^7 infectious unit per ml.

4.2.3 Surgery

See general methods.

refer to
general
methods

4.2.4 Auditory fear conditioning

See general methods.

refer to
general
methods

4.2.5 Cocaine-conditioned place preference

See general methods.

refer to
general
methods

4.2.6 Flourescent *in situ* hybridization

Tissue preparation

After behavioural experiments, animals were anaesthetized with isoflurane and decapitated. The brains were quickly dissected, frozen on dry ice, and stored in -80°C . At least 1 day after, the brains were taken out for slicing and equilibrated in the cryostat at the optimal cutting temperature (typically -20°C , with blades, brain matrix, mold, and mounting base. The brains were then cut on the brain matrix into 1 cm trunks containing the structure of interest. A thin layer of embedding medium () was added to the mold, and 4-5 brain trunks from different conditions were quickly mounted in the mold. The brains are sliced into $20\text{ }\mu\text{m}$ coronal slices and melt-mounted on Superfrost Plus slides (VWR). The slices were kept in -80°C until hybridization.

info about
OCT com-
pound

right way
to put this

Riboprobe synthesis

Template deoxyribonucleic acid (DNA) plasmids were linearized by restriction enzyme digestion at the 5'end of the target gene and purified. Riboprobes were synthesized using commercially available *in vitro* transcription kit () with digoxigenin (DIG) or flourescein labeling mix (). Turbo DNase were then added to the mixture, and incubated at 37°C for 15 min to remove the DNA template. The DNase was inactivated by 0.05 M ethylenediaminetetraacetic acid (EDTA). The riboprobes were purified by a ribonucleic acid (RNA) purification column (). A small sample of the riboprobes were taken out for quantification of the yield on a spectrophotometer (Absorbance at A_{260}) and run on a denaturing gel for confirming the integrity of the probe. The rest of the probes were stored in -80°C .

in vitro
transcrip-
tion detail

labeling
mix detail

RNA col-
umn info

Hybridization and staining

A selection of slides evenly distributed in A/P were selected to cover LA. The slides were thawed on a filter paper and loaded on an autoclaved metal rack. The slides were lightly fixed in cold 4% PFA for 10 min, then carried through fresh acetic anhydride solution (10 min), 2×saline sodium citrate buffer (SSC buffer) (5 min), 1:1 methanol/acetone (5 min), and 2×SSC buffer (5 min). The slides were then treated with prehybridization buffer (Sigma) for 30 min. The riboprobes were diluted to $0.67\text{ ng }\mu\text{l}^{-1}$, heated to 90°C for

prehyb
info

7 min and cooled on ice. Each slide was applied with 150 μ l riboprobe solutions, coverslipped, and incubated in a humid chamber overnight at 56 °C for hybridization.

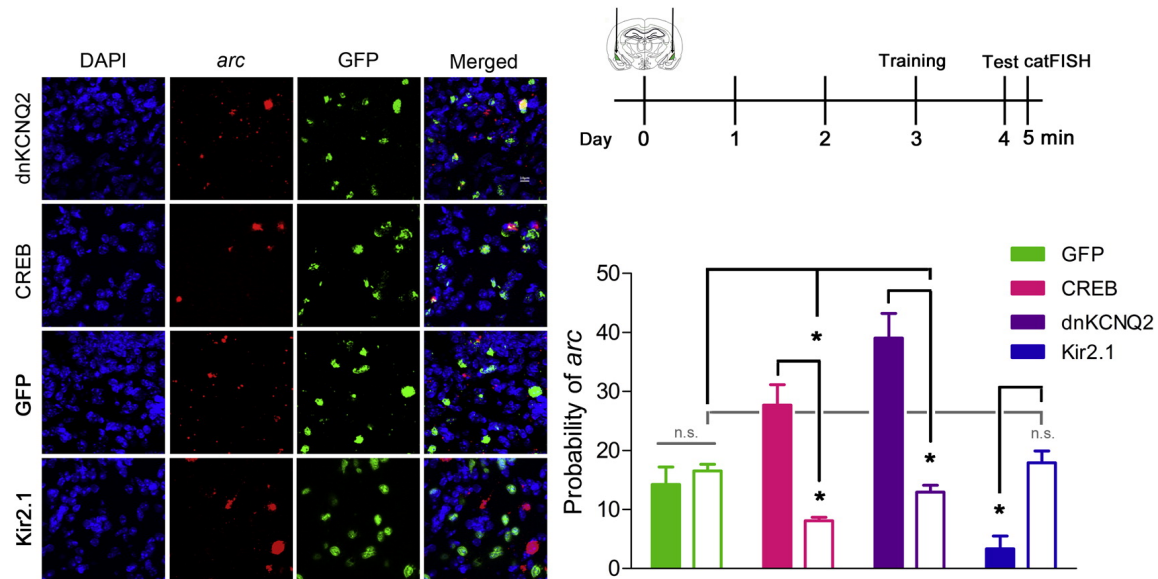
After hybridization, slides were treated with 1 ng ml⁻¹ RNase A at 37 °C for 30 min, washed with 2× SSC buffer, incubated 2 times with 0.5×SSC buffer at 56 °C for 30 min each, and washed with 2×SSC buffer. the slides were then incubated with blocking solution at room temperature for 30 min and then treated with Alexa-488 conjugated anti-GFP (1:100,) and horseradish peroxidase (HRP)-conjugated anti-DIG antibodies (1:300,) for 2 h to detect hybridized GFP and activity-regulated cytoskeleton-associated protein (Arc) RNA probes. The Arc signals were amplified using tyramide signal amplification (TSA)-biotin kit and stained by Alexa 568-conjugated streptavidin (1:300). The nuclei were counter-stained with Hoechst 33258.

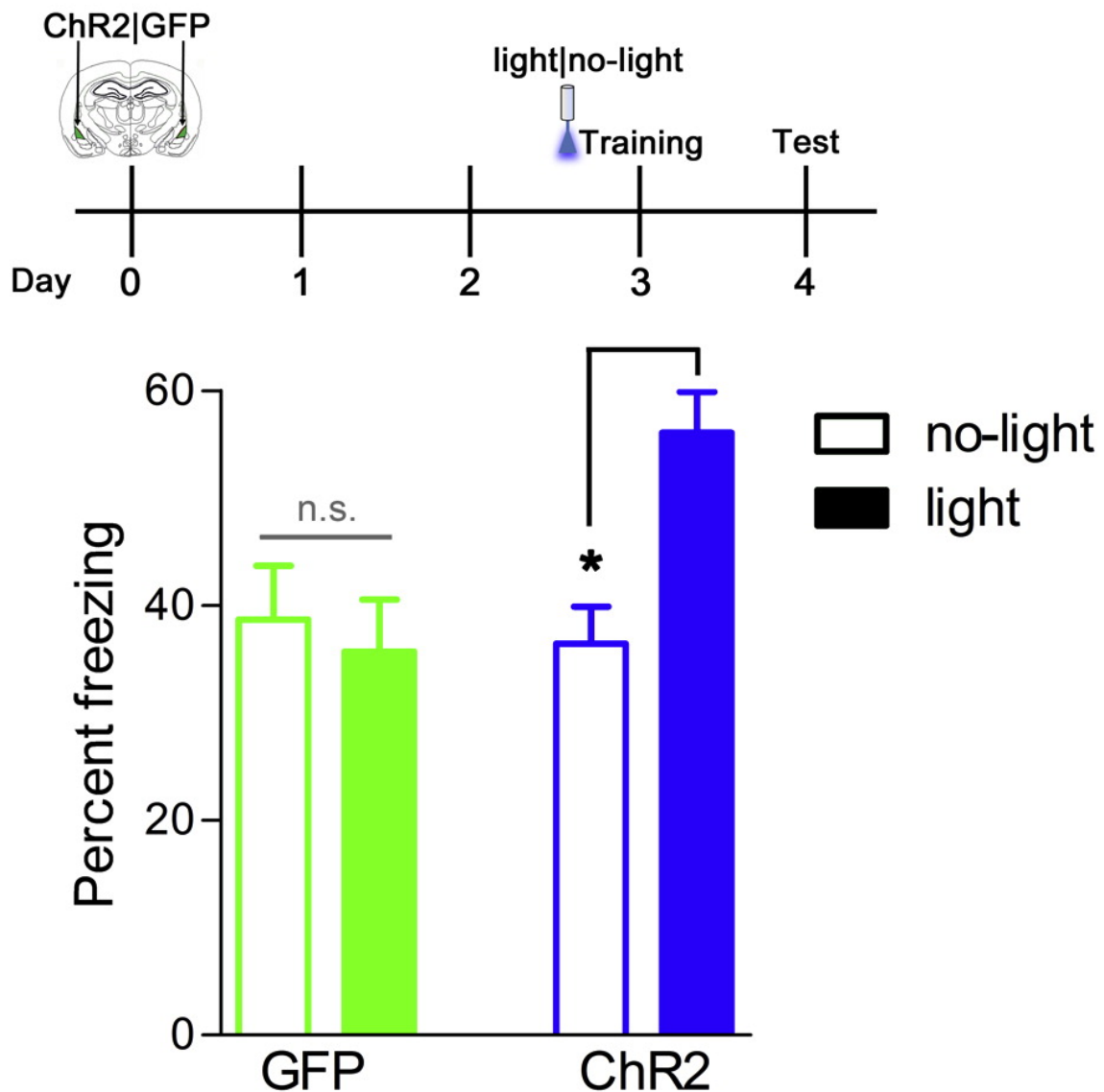
Ab info
Ab info

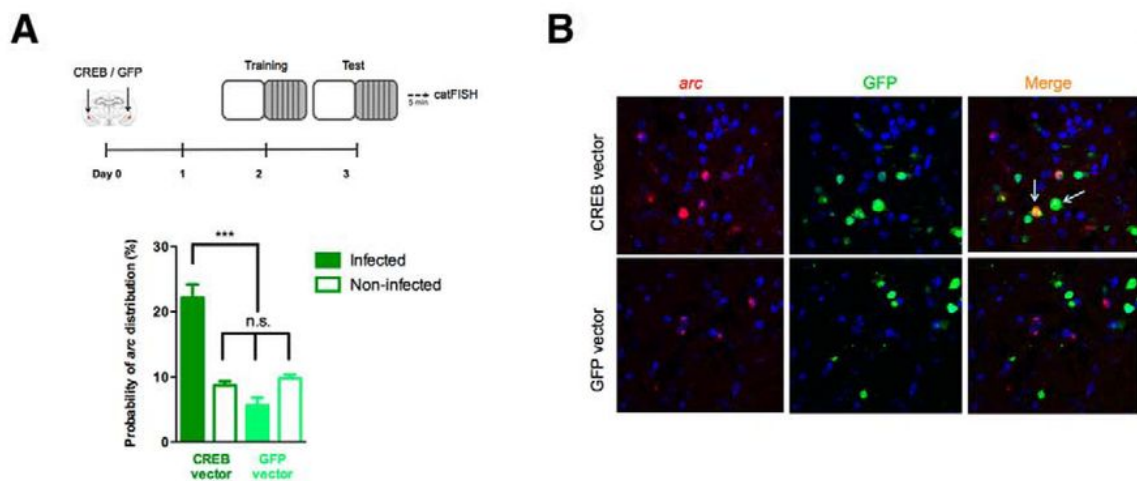
Analysis

Images were taken on a laser-scanning microscope. The parameters were optimized for Arc signal and kept constant across slides. Confocal stacks of 1um were taken by 40x objectives. Small-uniform nuclei from glial cells and nuclei on the top or bottom stacks were excluded from the counting. Nucleus immediately-early gene (IEG) signals are characterized by a double puncta that overlaps with nulei counter-staining.

4.3 Results







4.4 Discussion

5

CONSTRUCTION OF A MINIATURE EPI-FLUORESCENCE MICROSCOPE

5.1 Introduction

One of the major technological limitation in neuroscience research is recording neural activity in model animals. Traditional techniques such multi-unit recordings give excellent temporal resolution, however the spatial resolution — as measured by the number of cells simultaneously recorded — is limited. Moreover, it is very hard to distinguish cell subpopulations within the same region from the recording. Neural activity can also be inferred by post-hoc staining of neural activity markers, such as cfos or arc. This method give excellent spatial resolution, however the temporal resolution is very poor, where the time window of neural activity lasts from minutes to hours.

edit microscope intro

Live calcium imaging gives the best of both method. By labelling the cell of interest with a calcium indicator, neural activity can be inferred in milli-second resolution. Hundreds of cells can be simultaneously recorded, and specific subpopulations can be distinguished by fluorescence in different colour channels. However, traditional live calcium imaging requires the animals' head firmly fixed under a microscope stage. This requirement is incompatible with most well established behaviour assays, and at the same time introduce significant stress to the animal, potentially confounding the behavioural result. Moreover, due to light scattering in the opaque brain tissue, most of the studies have focused only on cortical areas, while techniques to image deep brain tissue on a standard two-photon microscope is still under development and not widely adopted (Barreto and Schnitzer, 2012).

In vivo calcium imaging in behaving animals is first demonstrated by Mark Schnitzer's group in Stanford (Ghosh et al., 2011). The authors constructed a miniature epifluorescence

microscope which is chronically implanted in the brain to image the fluorescence from region of interest. In a follow-up paper (Ziv et al., 2013), the authors demonstrated that the miniature microscope can image GCaMP3 calcium signals from hippocampal cornu ammonis area 1 (CA1) place cells for more than a month. However, there has been several limitations of their design: first their design incorporates an objective lens of 1 mm in diameter, which is impractical to reach deep brain tissue; second, their mini-microscope was only able to identify GCaMP signals, and therefore unable to distinguish different cell types within the population (Ghosh et al., 2011; Ziv et al., 2013).

In the current project, we aim to tackle the above mentioned limitations by building a head-mount miniature microscope which is able to image calcium signals in deep brain structures, while also able to image a separate fluorescence colour channel, allowing to distinguish difference cell type. The mini-microscope, once developed, will be used for imaging LA neurons to investigate mechanisms of fear memory encoding.

5.2 Material and Methods

5.2.1 Design of the mini-microscope

The mini-microscope has the same design as an general single-photon epifluorescence microscope except for the size constraints. Excitation light is emitted from a light-emitting diode (LED) light source, filtered, reflected by a dichroic mirror and evenly illuminate the sample. The fluorescent light from the sample is collected by the objective, passes through the dichroic mirror, filtered and focused on the camera. To fit the size constraints, we chose the use a high-intensity LED as the light source, a gradient-index (GRIN) lens as an objective, and a miniaturized complimentary metal-oxide-semiconductor (CMOS) camera to capture the image.

maybe a illustration

The optical design of the microscope is aided with Zemax software (Zemax Development Corporation) to optimize the lens and filter configuration. The casing of the microscope is modelled using OpenSCAD software.

Lens configuration

The lenses configuration consists a GRIN objective lens and a ocular cube lens forming a 4F system, where the distance between the thin-lens equivalent of the two lenses equals to the sum of the focal length. Potential lenses for emission light path are selected from modelling and calculation to give a working distance of 100 µm in water, a magnification of 6x and a back focal length of 6 cm. During prototyping, the lenses are purchased and installed into custom-made mounts on a two-arm stereotaxic frame. The distance of the lenses are then

optimized against a fibre bundle light source close to the GRIN lens. A drum lens is used to collect light from the LED. The drum lens is tested in a similar manner and selected to give diverging light after GRIN lens. We chose to use an achromatic doublet ($F=15\text{ mm}$, Edmund Optics). We used a 1.8 mm diameter 0.25-pitch GRIN lens (64-537, Edmund Optics) as objective for hippocampus imaging. To minimize brain damage for deep brain imaging, the objective lens was a home-assembled doublet of a 0.5 mm diameter, 1-pitch GRIN relay lens () and a 2 mm diameter 0.25-pitch GRIN lens (). The details of doublet assembly is described in .

GoFoton
lens info

GoFoton
lens info

Filter selection

The filters are selected to cover the excitation and emission spectrum of the genetic encoded calcium sensor GCaMP6s (Chen et al., 2013), and further screen for high bandwidth and low overlap. The fit the size constraints, the excitation and emission filters had dimensions of $5\text{ mm} \times 5\text{ mm} \times 1\text{ mm}$, and the dichroic mirror $7.1\text{ mm} \times 5\text{ mm} \times 1\text{ mm}$. We chose to use a fluorescein isothiocyanate (FITC) filter set for gCaMP6 imaging (). For dual colour imaging, we took advantage of significant long tail of the red retrobeads spectrum, and use the same blue light to excite the red fluorophore. In these experiments, a TRITC/FITC filter set was used ().

chroma
filter info

chroma
filter info

Electronics

The image sensor are selected to have an packaged size of less than $1.5\text{ cm} \times 1.5\text{ cm}$. We used a commercially available analogue camera module (HD1313BW, Ruishibao) that gives satisfactory sensitivity and dynamic range. The camera board is connected to a 5 V power regulator. After the power regulator, the wires were connected through a slip ring () was the used to avoid tanglement of the wires during animal behaviour. After the slip ring, the wires are connected to a 12 V direct current (DC) power source and a universal serial bus (USB) analogue video capture card (). The video capture card is controlled by custom software for synchronized video capture (See code in).

slipring
info

Video cap-
ture info

reference
code

led info

DC power
source info

Casing and assembly

The casing model is produced by 3D printing using PolyJet technology with VeroBlackPlus material (Stratasys). This gives a rigid, opaque and black casing with highest resolution

for details. The microscope body is screwed onto the camera holder via M8 thread to allow easy change of the focus plane. A side M2×2 mm nylon screw () is used to lock the camera holder on the microscope body.

info side screw

A metal nut was glued to the bottom of the microscopy body concentric to the light path opening using a fast-curing epoxy glue (). The nut allows to easily and firmly lock the microscope onto the baseplate.

microscope body nut spec

epoxy info?

baseplate thread tube info

Unlike the microscope body, the base plate was 3d printed using fused deposition modelling (FDM) with polylactic acid (PLA) material. A threaded tube () was heated with a soldering iron and inserted into the center of the base plate, and further fixed with epoxy glue. The objective lens was inserted into the center of the threaded tube, and fixed with crazy glue on the bottom. For objective that are thinner than the inner diameter of the threaded tube, an additional stainless steel tube was inserted inbetween to aid alignment of the lens.

Objective lens assembly for deep brain imaging

For deep brain imaging, a 0.5 mm diameter, 1.0-pitch relay lens was glued to a 2 mm diameter, 0.25-pitch GRIN lens. The setup is modified from (Kim et al., 2012) to ensure concentricity and alignment. In the setup, a V-groove clamp (, ThorLab) is used to hold the large GRIN lens in place vertically, and the thin relay lens was mounted on another V-groove clamp attached to a 3-axis manipulator (, ThorLabs). The two V-groove clamps were leveled using a bull's eye spirit level. An analogue lens and camera chip was mounted under the large GRIN lens, and displayed the image of the large GRIN lens on a monitor. A dissecting microscope was mounted horizontally for monitoring the vertical position of the two lenses.

clamp details

manipulator details

insert fig-
ure for the
setup

During assembly, both lenses were mounted in the V-groove clamps respectively. A small drop of ultraviolet (UV) curing optical adhesive (NOA61, Norland) was added to the bottom surface of the relay lens using a 27-gauge needle. The relay lens was then lower to just above the large GRIN lens when an image of the relay lens is visible on the monitor. The relay lens was then moved to the center of the large GRIN lens according to the monitor display. Observed through the dissecting microscope, the relay lens was then lowered to touch the upper surface of the large GRIN lens. A 375 nm spot UV light source () was used to cure the optical glue. The curing time is calculated to give at least 3 J mm^{-2} of UV light on the optical adhesive.

uv light
source info

5.2.2 Implantation of the mini-microscope

Two weeks after gCaMP6 infusion to the target area, animals are anesthetized and head-fixed on a stereotaxic frame as described in . Three screws were placed around the viral injection site for anchoring the microscope.

ref general methods

For implantation targetting CA1, a circular craniotomy of 2 mm was performed above the viral injection site. The dura was pierced and lifted with a fine tweezer to expose the brain. The brain is then constantly irrigated with artificial cerebral-spinal fluid to remove the blood. A 27-gauge aspiration needle was used to remove cortex and expose CA1. For implantation targetting amygdala after anchoring the screws, a 27-gauge needle was lowered to the target coordinate, left for 5 min, and slowly retracted.

The mini-microscope is then fixed on the stereotaxic frame and gradually lowered to the target coordinates (CA1: LA:). Opaque black dental acrylic was used to secure the microscope baseplate to the skull. Once the dental acrylic cured, the microscope body was detached from the baseplate and replaced with a cap. Animals were given 5 mg kg^{-1} ketoprofen for analgesia.

coordinate for ca1 and amygdala

5.2.3 In vivo mini-microscope testing

After lens implantation, the animals were kept in the home cage for at least two weeks before the first image session. This time allows the optical window to clear up. The animals were scruffed, the cap was removed and replaced with the microscope body. A typical imaging session lasts for 5 min. After the imaging session the microscope body was removed, and the animal was recapped.

5.2.4 Image analysis

Illumination correction

illumination correction meth

Motion correction

motion correction meth

Extracting cell from calcium imaging video

Individual cell calcium signals were extracted from the movie as previously described (Mukamel et al., 2009). Briefly, we first estimate the number of cells in the movie, and reduced the number of temporal dimension to roughly number of cells using principle component analysis. The resulting principle components were then subjected to independent

component analysis, where the spatial filter for individual cells were extracted from the components, and the calcium signal of the corresponding cell was extracted from the mixing matrix. The time-course calcium signal was then aligned with behaviour recordings to identify neural activity patterns.

Mapping cells across session

Cells are extracted from the recordings for both session respectively. The position of the each cells were calculated as the center of mass of the 90 percent pixels in the extracted independent component analysis (ICA) component. The position of cells for each recording were approximately aligned to have overlapping center of mass, then rotated to have overlapping principle component vectors. The two point clouds are then precisely aligned using TrimICP(). TrimICP is robust against outliers, which can be observed even when cells fire in one session but were silent in another. TrimICP was performed using a 40% outlier ratio, optimizing both translation and rotation. After alignment, cells that are less than 5 μm from one session to another are mark as same cells.

ref Trim-
ICP

5.3 Results

5.3.1 mini-microscope

The mini-microscope provides a cheap and easy way for neuroscience laboratories to measure calcium activity in freely behaving small animals. The completely assembled mini-microscope weighs less than 3 g, and can be bounded in a 25 mm \times 16 mm \times 11 mm box (Figure 5.2b). Adult mice with the mini-microscope attached are able to rear, groom, and freely explore environment with no noticeable change from their natural behaviour ().

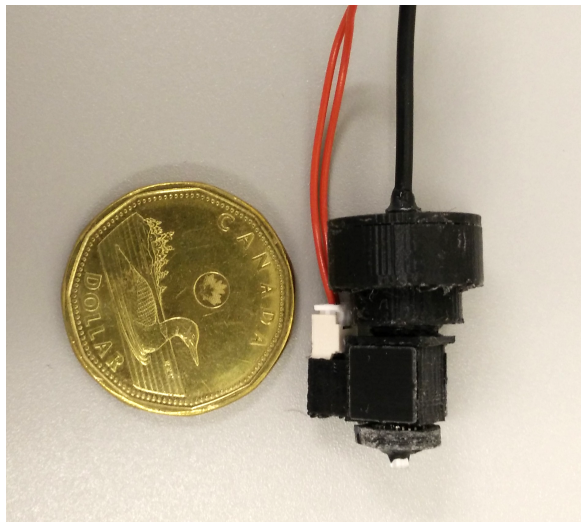
mouse im-
age?

The theoretical optical resolution of the mini-microscope is 1 μm . To measure the resolution empirically, we tested the mini-microscope against United States Air Force (USAF) resolution target (, Edmund Optics). As shown in Figure 5.2c, the thinnest lines (group 7 element 6, 2.07 μm width) are clearly visible. This suggest that the empirical resolution of the microscope is smaller than 2 μm . With this resolution, the mini-microscope is able to resolve cell bodies and capillary blood vessels.

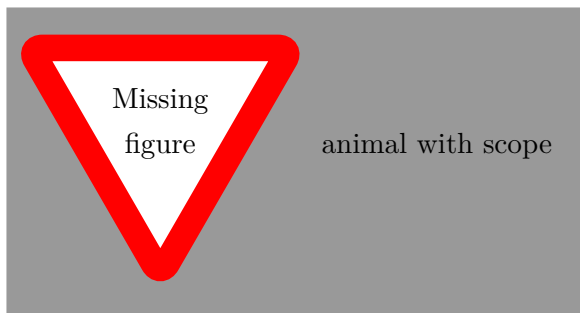
insert mi-
croscope
photo and
mouse fig-
ure here

In order to test the illumination, we expressed GFP in LA of an animal, perfused and harvested the brain 3 days later when the HSV expression peaks. The brain was sliced coronally on a vibratome until the area of infection. The trunk of the brain was imaged under the mini-microscope. As seen is Figure 5.2d, the GFP cells are clearly visible. Moreover, many of the apical dendrites can also be resolved. The imaging quality is comparable

USAF tar-
get detail



(a)



to that taken under a standard epi-fluorescence microscope (Nikon . The imaging quality is lower than normal due to the thickness of the brain trunk). This result confirms that the fluorescence under the LED illumination can be reliably detected by the CMOS camera.

- Nikon details
- insert Nikon image
- reorganize figures

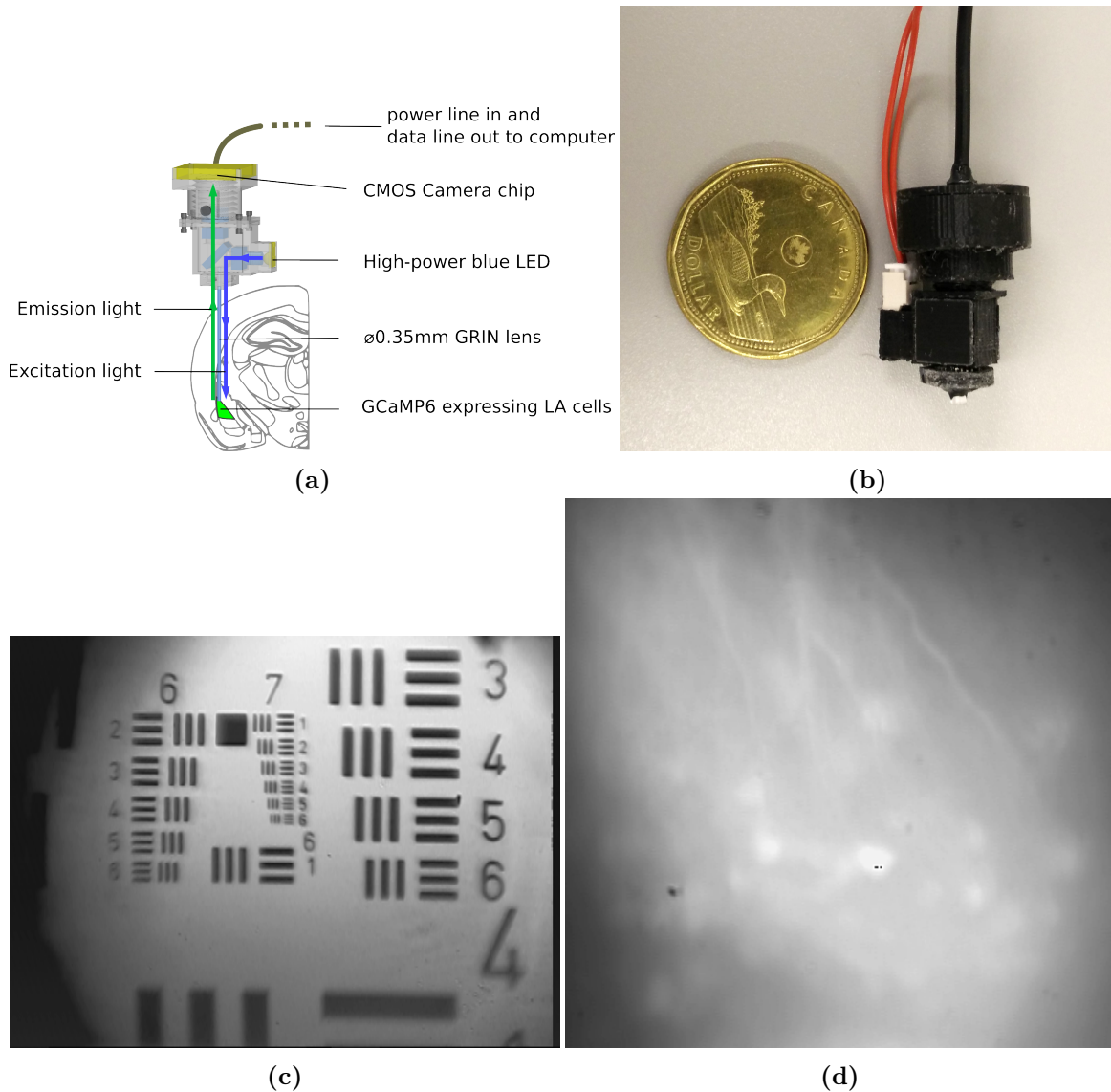


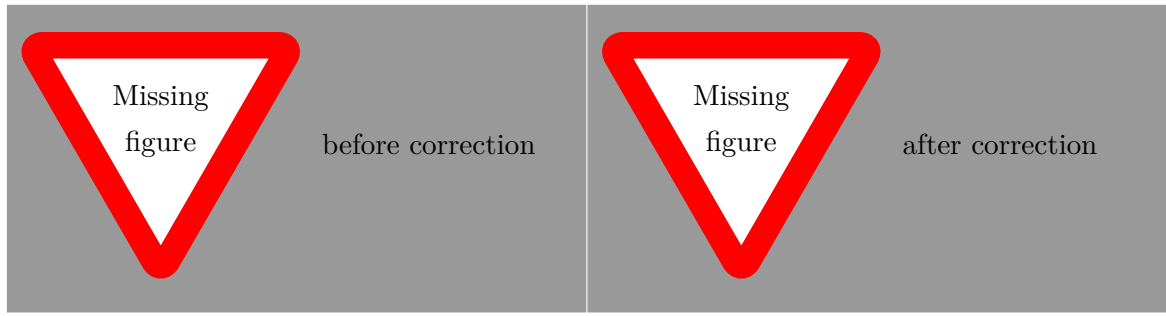
Figure 5.2. (a) Schematic of the miniature microscope. Excitation light is emitted from a high-intensity blue LED, filtered and reflected to the sample by a dichroic mirror. GCaMP6 emission is collected by the gradient-index (GRIN) lens, filtered and focused onto a CMOS camera chip, where the images are sent to a computer and recorded. (b) Prototype of the mini-microscope. (c) USAF resolution test target under the mini-microscope. (d) GFP-expressing cells in perfused brain under the mini-microscope.

5.3.2 Video preprocessing

illumination correction

Due to the size limitation of the mini-microscope, the illumination has to be compromised and is uneven. The uneven illumination not only affects the calcium signal and cell detection, but also adds difficulty to the motion correction step, since the uneven illumination pattern appears stable even when there is relative movement between the mini-microscope and the target. To correct this, a 2D gaussian filter with large window (15×15) is convolved with each frame to extract the illumination pattern. The illumination pattern is then subtracted from the frame. Figure 5.3 shows the maximum projection of the recording before and after illumination correction. Cells under intense illumination in the center can be clearly visualized after illumination correction.

move to methods?



... and normalized by multiplying the inverse of the difference of illumination pattern to roof

image

Figure 5.3. , before, after

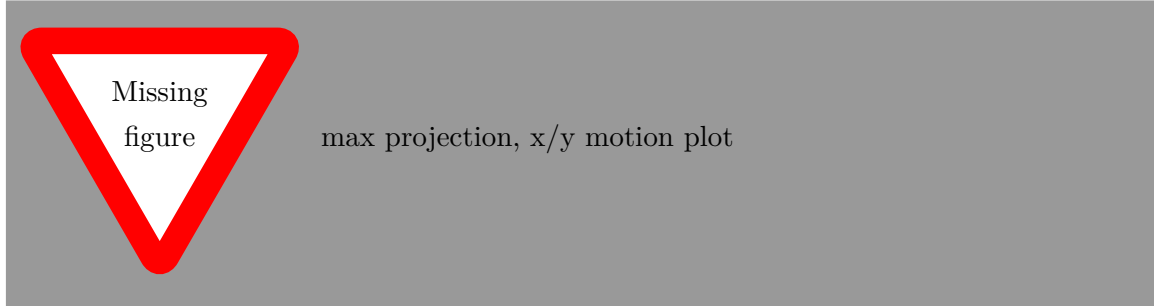
motion correction

After illumination correction, the movie was then removed from dust, and corrected for motion. Occasional dust speckles on the camera appears as stationary small dark objects in the movie, and would interfere with motion detection. To remove the dust speckles, for each frame, pixels two standard deviation darker than mean intensity are labeled. The labeled pixels are morphologically eroded and dilated to remove noise, and then inpainted using Navier-Stokes based methods () .

reference
opencv?

As the motion is almost entirely translational, after dust removal we used phase correlation algorithm to achieve sub-pixel level motion correction. The reference frame is initialized to be the first frame. A moving average of 25 registered frames were generated, and the reference frame is updated by maximum projection of the moving average frame to the reference frame. To test the efficacy of the motion correction algorithm, we have generated a particularly shaky recording by losing the connection of the mini-microscope

to the baseplate. As can be seen from the maximum projection of the original recording and stabilized recording (Figure), the motion correction works well even for extremely erratic motion.



5.3.3 Measuring blood flow with mini-microscope

To test *in vivo* imaging capability of the microscope, we first implanted the microscope above the cortex, and injected 150 µl of fluorescein-dextran (molecular weight 120 kDa). The fluorescein-dextran will fill the blood vessels and have similar excitation and emission wavelength to GCaMP. As expected, after fluorescein-dextran injection, the blood vessels are clearly visible when the microscope is implanted (Figure 5.4).

calculating
blood flow

image,
blood ves-
sel de-
tection,
velocity
heatmap

A vertical orange line connects the text "calculating blood flow" and "image, blood vessel detection, velocity heatmap" to the word "Figure" in the sentence above.

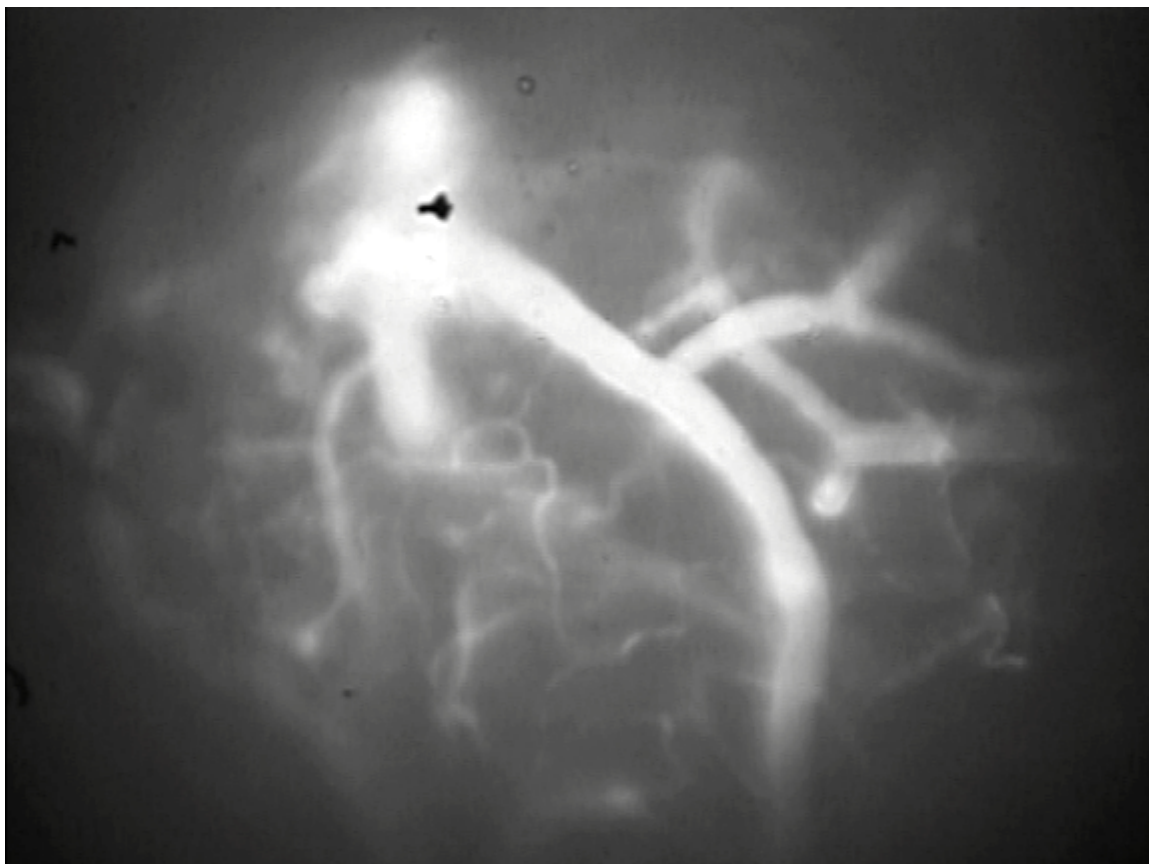


Figure 5.4. *In vivo* image of blood vessel. The animal received 10mg/kg fluorescein-dextran in tail vein. The mini-microscope is placed at cortex when the animal is under anaesthesia.

5.3.4 Recording calcium transients in CA1

To test GCaMP6s expression *in vivo*, we infused AAV-syn-GCaMP6s-WPRE into CA1 hippocampus and implanted the mini-microscope above the injection site. During behavioural session, the animal was placed in a novel environment to explore for 5 min, during which GCaMP6 fluorescence were recorded. The maximum projection of the GCaMP6 fluorescence in a 5-minute session is shown in Figure 5.5. We were able to extract 200 cells from the recording and their corresponding Ca^{2+} transients (Figure 5.75.6).

The positions of the animal was traced out in the behaviour video. The timecourse of the identified cells were mapped back to the behaviour of the animal. Figure 5.8 shows Ca^{2+} activity of potential place cells as they respond to specific location in the environment the animal is in.

max projection,
sample cell, animal tracking, place cell heat map

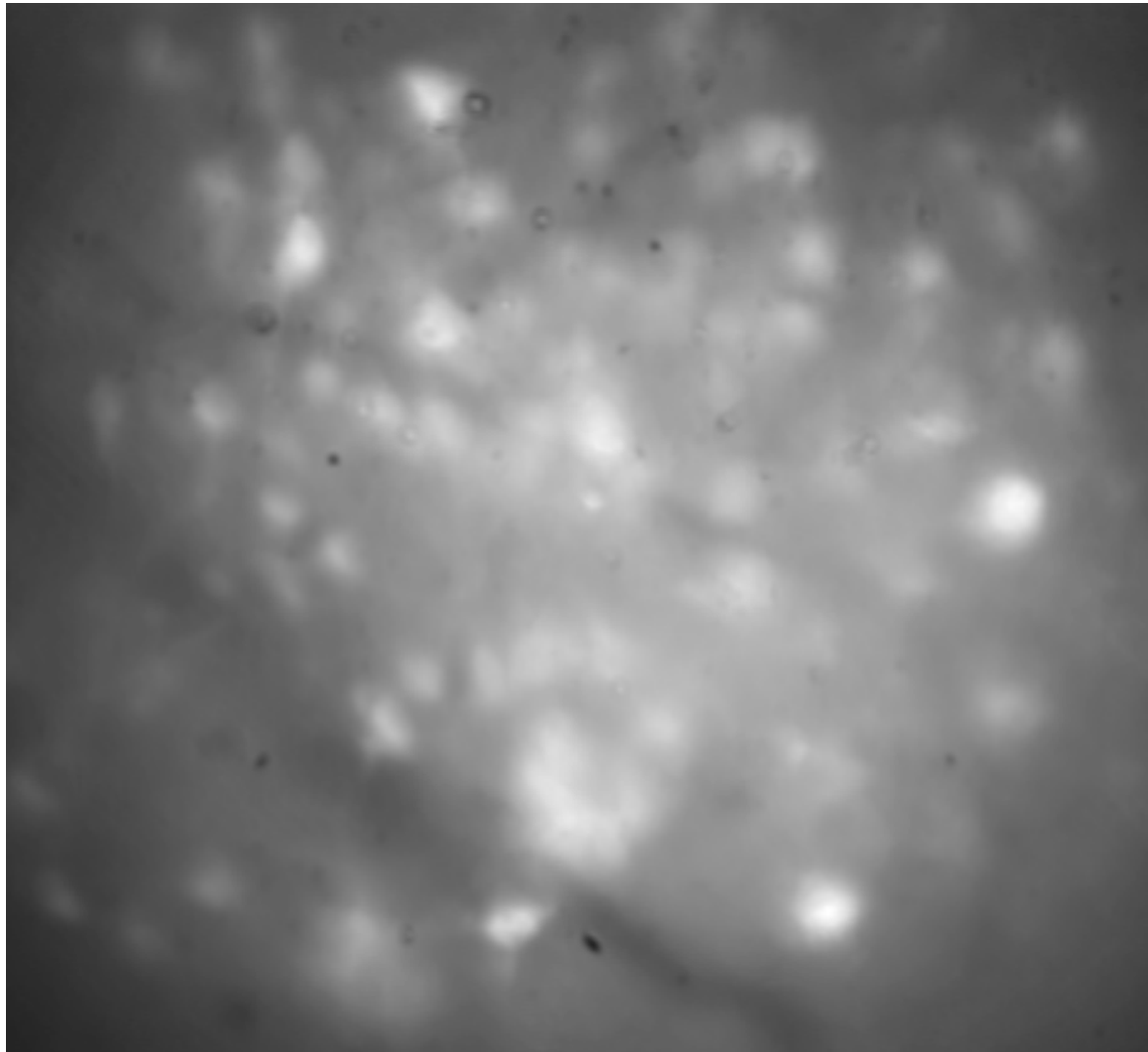


Figure 5.5. Cells in CA1 captured by the mini-microscope in behaving animal. Two weeks after AAV infusion and microscope implantation, the animal is allowed to freely explore a novel environment. The picture is a maximum projection of all frames captured in a 5-minute session.

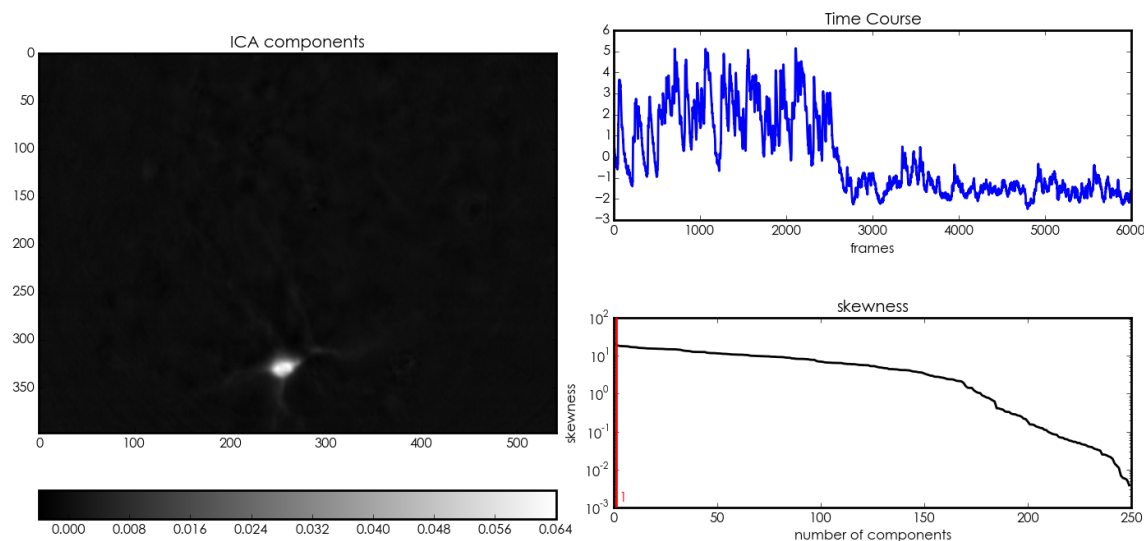


Figure 5.6. Example of an independent component of the movie after analysis, showing both the extracted spatial location of the cell (left) and the un-normalized activity (top right).

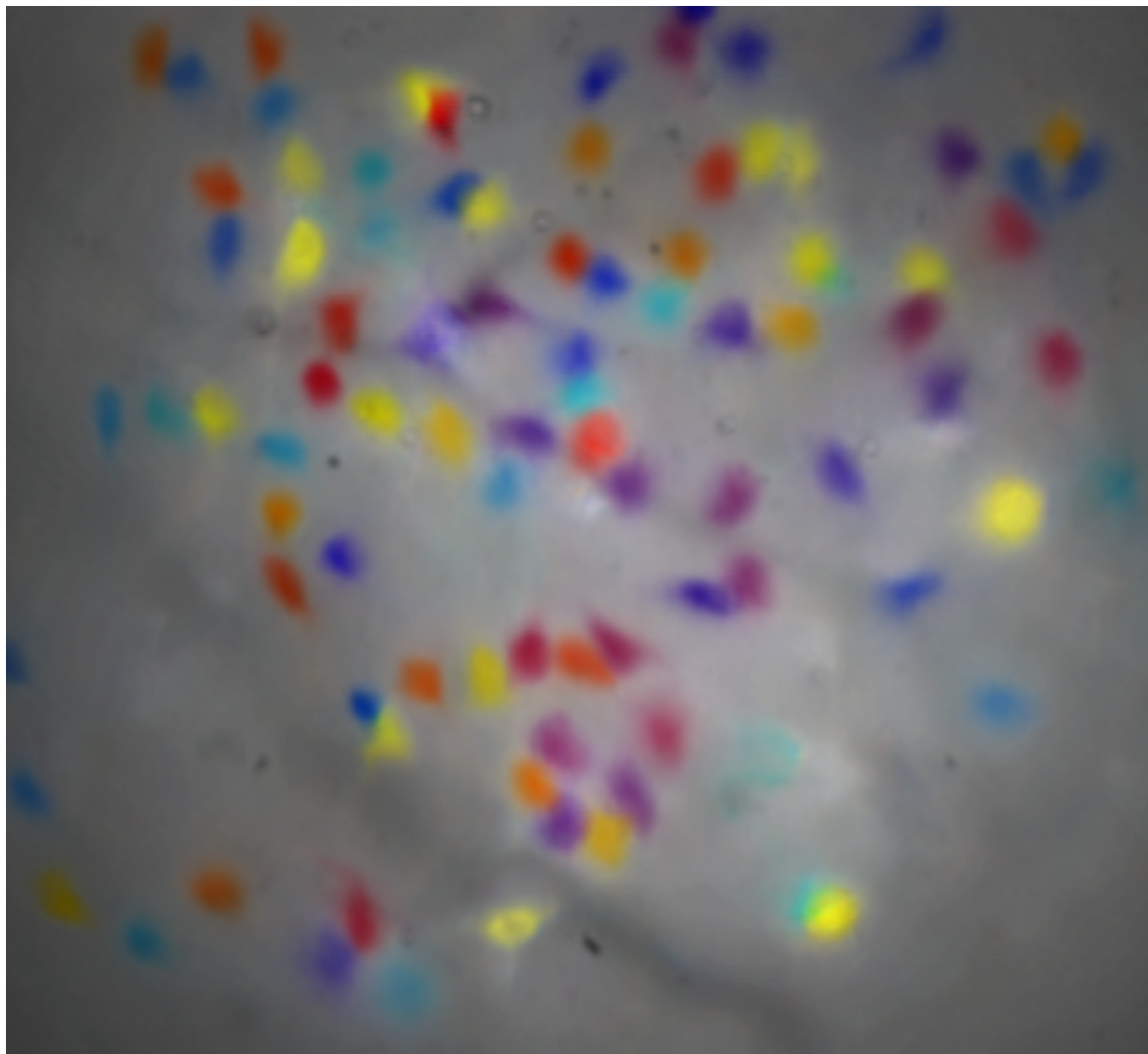


Figure 5.7. More than 100 cells are identified in a single imaging session. The identified cells are randomly coloured.

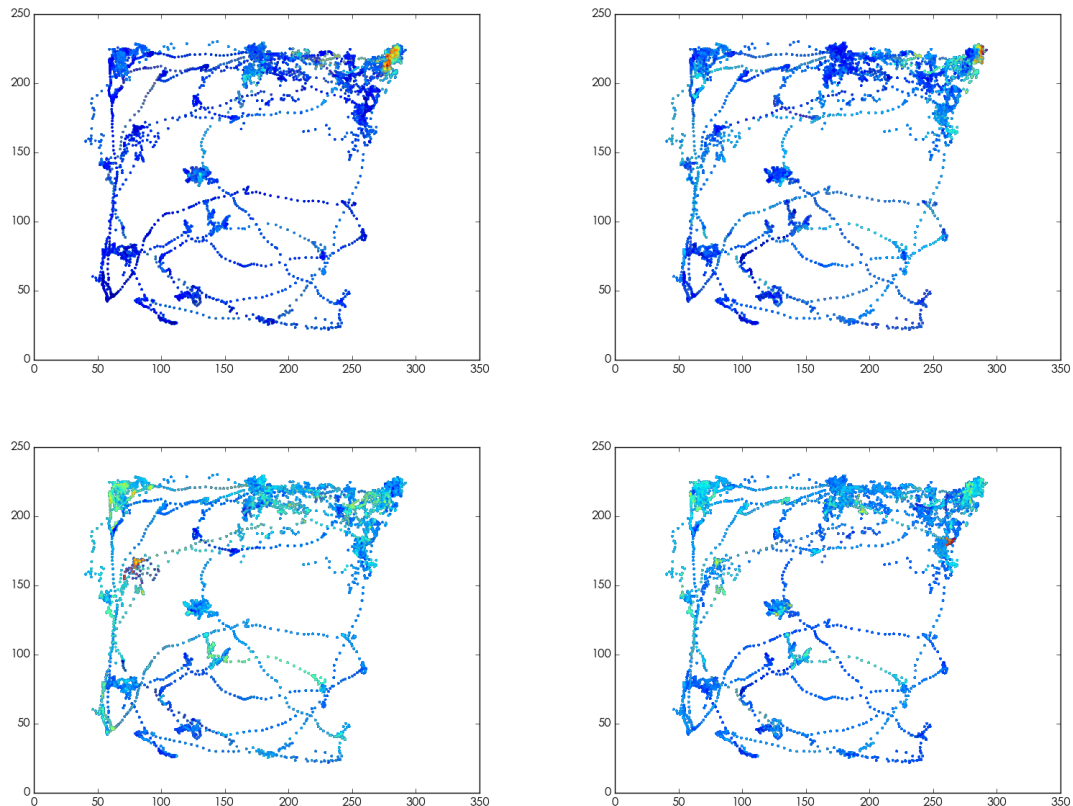


Figure 5.8. Activity of 4 sample cells plotted against location of the animal. The colour represents the Ca^{2+} activity. The cellular activity is specific to the animal's location in the environment.

5.3.5 between session stability

To measure the stability of the imaging field between sessions, animals with gCaMP6 infused in CA1 underwent contextual fear conditioning, and 24 h later, were put back to the same context for testing. Mini-microscope was attached during both imaging sessions, and the recordings are aligned as shown in .

5.3.6 Deep brain imaging

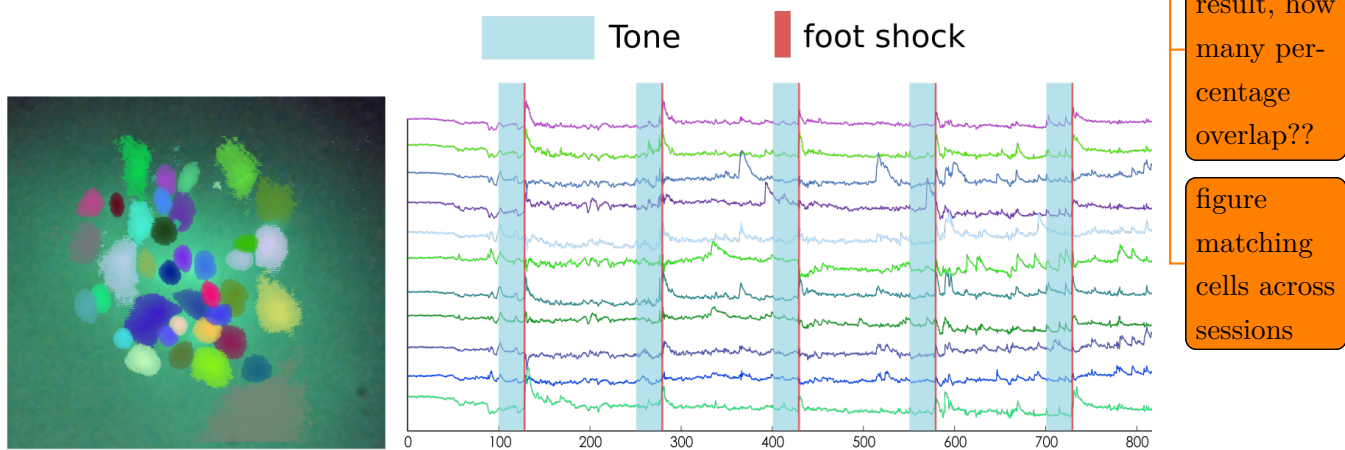


Figure 5.9. Raw calcium signals during fear conditioning. Left: extracted map of neurons, randomly coloured. Right: Sample calcium signals over time.

This design of the miniature microscope incorporates an objective lens of 1.8 mm in diameter. This lens is both too thick and too short to reach deep brain structures such as amygdala. We have modified the design and attached a 4.8 mm long 0.5 mm diameter relay GRIN lens (ILW-050-P050, GoFoton) to the objective lens. Attaching the relay lens does not significantly alter the imaging ability of the microscope, however allows the lens to reach deep brain regions without extensive damage. With this configuration, we are able to visualize activity from more than 40 cells in lateral amygdala and track them over time (Figure 5.9).

same as CA1 analysis

5.3.7 Two colour

To test the two-colour version of the mini-microscope, we infused red retrobeads () in nucleus accumbens (NAc) bilaterally and gCaMP6 adeno-associated virus (AAV) in LA. The retrobeads will be trafficked retrogradely along axons, and will label LA neurons that project to NAc. The images acquired from both the green and red channel are shown in Figure 5.10c,5.10d. There is no interference between the two channels.

retrobeads info

wording

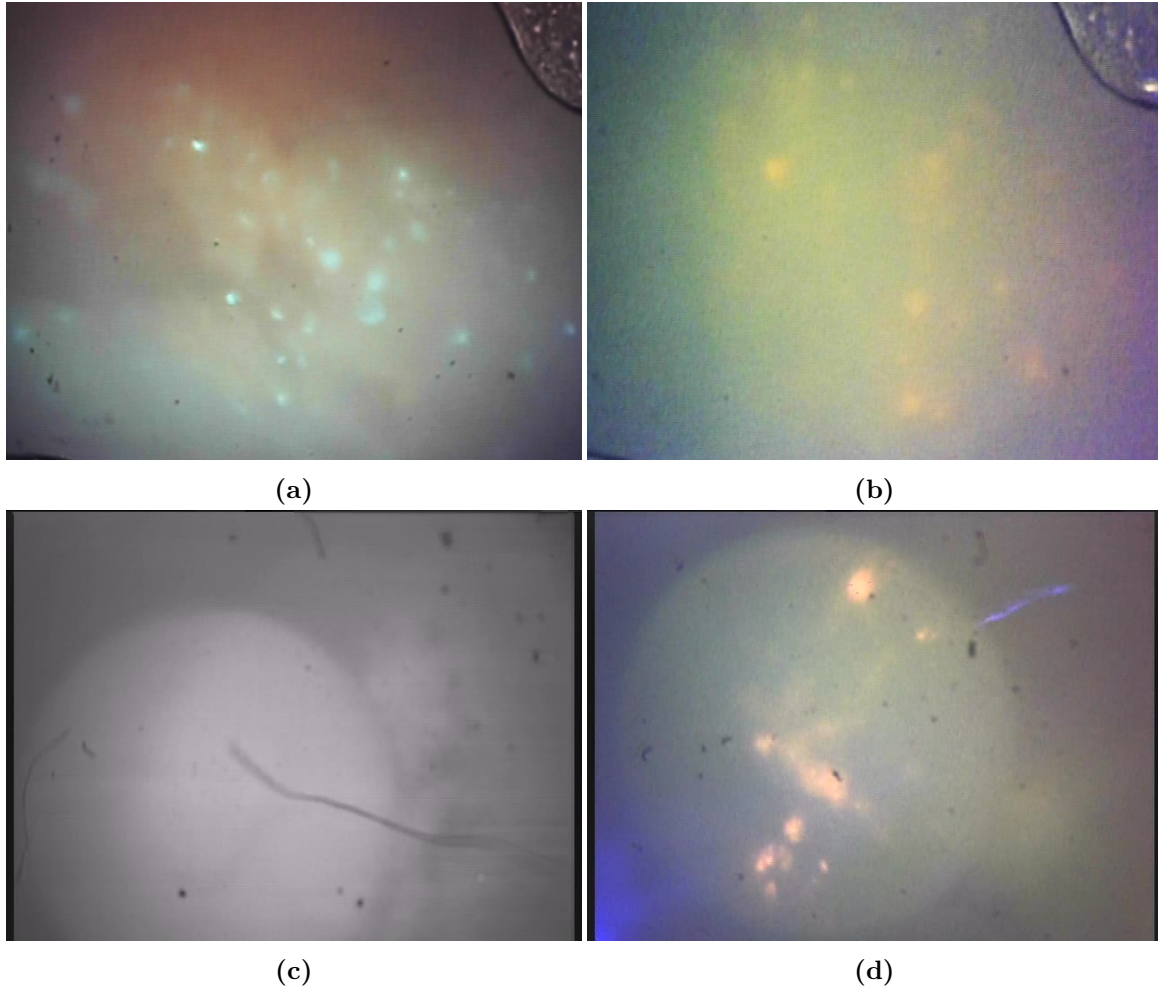


Figure 5.10. Images of cells with different fluorescent protein under the two-colour mini-microscope prototype. (a) HSV-GFP in perfused brain. (b) HSV-tdTomato in perfused brain. (c) Red retrobeads *in vivo* in green channel. (d) Red retrobeads *in vivo* in red channel.

5.4 Discussion

1-2 pages

6

DYNAMICS OF NEURAL NETWORK IN AMYGDALA DURING MEMORY FORMATION

7

GENERAL DISCUSSION

20 pages

8

CONCLUSIONS AND FUTURE DIRECTIONS

4-5 pages

BIBLIOGRAPHY

- Barretto, R. P. J. and Schnitzer, M. J. (2012). In vivo optical microendoscopy for imaging cells lying deep within live tissue. *Cold Spring Harbor Protocols*, 2012(10):1029–34.
- Chen, T.-W., Wardill, T. J., Sun, Y., Pulver, S. R., Renninger, S. L., Baohan, A., Schreiter, E. R., Kerr, R. A., Orger, M. B., Jayaraman, V., Looger, L. L., Svoboda, K., and Kim, D. S. (2013). Ultrasensitive fluorescent proteins for imaging neuronal activity. *Nature*, 499(7458):295–300.
- Ghosh, K. K., Burns, L. D., Cocker, E. D., Nimmerjahn, A., Ziv, Y., Gamal, A. E., and Schnitzer, M. J. (2011). Miniaturized integration of a fluorescence microscope. *Nature Methods*, 8(10):871–8.
- Kim, J. K., Lee, W. M., Kim, P., Choi, M., Jung, K., Kim, S., and Yun, S. H. (2012). Fabrication and operation of grin probes for in vivo fluorescence cellular imaging of internal organs in small animals. *Nature protocols*, 7(8):1456–69.
- Mukamel, E. A., Nimmerjahn, A., and Schnitzer, M. J. (2009). Automated analysis of cellular signals from large-scale calcium imaging data. *Neuron*, 63(6):747–60.
- Neve, R. L., Neve, K. A., Nestler, E. J., and Carlezon, W. A. (2005). Use of herpes virus amplicon vectors to study brain disorders. *BioTechniques*, 39(3):381–91.
- Ziv, Y., Burns, L. D., Cocker, E. D., Hamel, E. O., Ghosh, K. K., Kitch, L. J., El Gamal, A., and Schnitzer, M. J. (2013). Long-term dynamics of ca1 hippocampal place codes. *Nature Neuroscience*, 16(3):264–6.

A

APPENDIX

A.1 Code